

КРАТКИЕ СООБЩЕНИЯ

UDC 541.6:547.12:546.28

A COMPARATIVE STUDY OF THE RADIAL DISTRIBUTION OF HYDROGEN ON C₂₀, C₁₉Si, AND C₁₉B CAGE FULLERENES: A MONTE CARLO SIMULATION

F. R. Nikmaram

Department of Chemistry, Faculty of Science, Yadegar-e-Imam Khomeini (RAH) Branch, Islamic Azad University, Tehran, Iran

E-mail: Nikmaram87@yahoo.com, Nikmaram88@iausr.ac.ir

Received January 16, 2015

The radial distribution of hydrogen on C_{20(cage)} and C₁₉Si_(cage), and C₁₉B_(cage) fullerene structures is investigated at different temperatures (273, 293, 320, and 400 K) for the pressure range between 1 MPa and 30 MPa using the (N,V,T) Monte Carlo simulation. The gravimetric storage capacity and radial distribution function parameters show that, under the identical temperature and pressure conditions, the magnitude of the hydrogen radial distribution on the C₁₉B surface is larger than that on C₁₉Si and C₂₀. The calculated maximum of the gravimetric storage capacity for C₁₉B at 273 K and 30 MPa is 7.6 %.

DOI: 10.15372/JSC20160321

Keywords: boron, silicon, C₂₀ fullerene, H₂ radial distribution, Monte Carlo.

In general, energy conversion and storage systems require a rather complex combination of materials that can selectively promote an adsorption process with efficiencies close to the thermodynamic limit [1]. Pure hydrogen can be the final destination in the evolution of fuel usage from coal to petroleum to natural gas, which has followed a trail of increasing hydrogen content [2]. A major bottleneck for the hydrogen vehicle is the problem of hydrogen storage. Hydrogen has the highest energy per unit mass but occupies a large volume. Even in the liquid form, the energy density of hydrogen is only 8.4 MJ/L, compared to 34.2 MJ/L for gasoline. Hydrogen has been recognized as an ideal energy carrier with a heating value three times higher than that of petroleum [3]. However, several studies have been performed to meet the goals of the U. S. Department of Energy (DOE) Hydrogen plan, 6.5 wt% (weight percent), most of them have failed to approach the proposed target. Recently, considerable attention has been driven to porous materials such as clathrates, zeolites, carbon nanotubes, and fullerenes as possible materials for hydrogen storage [4].

The properties of silicon and boron substituted fullerenes have motivated a number of studies in recent years on SiC fullerene and boron fullerene type structures [5, 6]. Boron and silicon-doped carbon clusters of the types B_mC_n (m = 1–4) and Si_mC_n (m = 1, 2) have been produced via the laser-vaporization cluster beam technique [7].

C₂₀ is regarded as the smallest experimentally synthesized carbon fullerene with 12 pentagons [8].

Model and simulation details. In this work, the radial distribution of hydrogen on C_{20(cage)}, C₁₉Si_(cage), and C₁₉B_(cage) fullerene structures have been investigated at different temperatures (273, 298, 320, and 400 K) for the pressure range between 1 and 30 MPa, using the (N,V,T) Monte Carlo simulation by the Lennard—Jones (LJ) 12-6 potential ($\Phi_{LJ(r)}$) [9]

$$\Phi_{LJ(r)} = 4\varepsilon_{gc}[(\sigma_{gc}/r)^{12} - (\sigma_{gc}/r)^6], \quad (1)$$

where r is the distance between the gas molecules and surface atoms in the fullerene structures; σ_{gc} denotes the LJ gas-fullerene collision diameter; and ε_{gc} is the LJ gas-carbon potential well depth. The Lennard—Jones parameters for the interaction between the gas and fullerene surfaces were calculated using Eqs. (2), (3) [10—12]. We have considered these parameters for Si—C, C—C, B—C, H₂—H₂, C—H₂, Si—H₂ and B—H₂ pairs [13—18].

In our simulations, periodic boundary conditions are imposed in all directions. A cubic simulation box (50.0, 50.0, 50.0 Å) contains one fullerene structure and H₂ molecules. The cutoff length in evaluating the LJ potential is set to 2.5 Å on all fullerene structures.

$$\varepsilon_{ij} = \sqrt{\varepsilon_i \varepsilon_j}, \quad (2)$$

$$\sigma_{ij} = \frac{(\sigma_i + \sigma_j)}{2}. \quad (3)$$

For each calculation, 10⁷ configurations are generated. The initial configurations are discarded to guarantee equilibration, whereas the remaining configurations are used as the average of the desired ensemble properties. The effects of the temperature and pressure on the adsorption phenomena are examined.

The aim of the present work is the presentation and comparison of the gravimetric storage capacity (absolute value adsorption per mass of adsorbent, ρ_w) and the radial distribution function (RDF) parameters for the structures. The gravimetric storage capacities on the basis of hydrogen absorption are comparable for all three structures.

The gravimetric storage capacity ρ_w was calculated by Eq. (4)

$$\rho_w = \frac{N_{\text{gas}} m_{\text{gas}}}{N_{\text{gas}} m_{\text{gas}} + N_c \cdot m_c + N_{\text{hetero}} m_{\text{hetero}}}, \quad (4)$$

where N_{gas} , N_c , and N_{hetero} are the number of gas molecules outside the fullerene structure up to 2.5 Å, the number of carbon atoms in the simulation box, and the number of heteroatoms (=1), and m_{gas} , m_c , and m_{hetero} (g/mol) are the corresponding molar masses, respectively [19].

Results and discussion. The radial distribution of H₂ on C_{20(cage)}, C_{19Si(cage)}, and C_{19B(cage)} fullerene structures at 273, 293, 320, and 400 K for the pressure range between 1 and 30 MPa is studied by the (N, V, T) Monte Carlo molecular simulation and fitted by the Lennard—Jones potential equation. Figs. 1, 2, and 3 show the radial distribution function of H₂ adsorption on C₂₀, C_{19B}, and C_{19Si} with respect to r at 273 K as a sample.

The temperature and pressure of maximum RDF for the structures are listed in Table 1. Table 1 shows that maximum RDF are 0.01607, 0.01906, and 0.02018 at 3 Å, 273 K, and 25 MPa for C₂₀, 20 MPa for C_{19Si}, and 30 MPa for C_{19B} respectively.

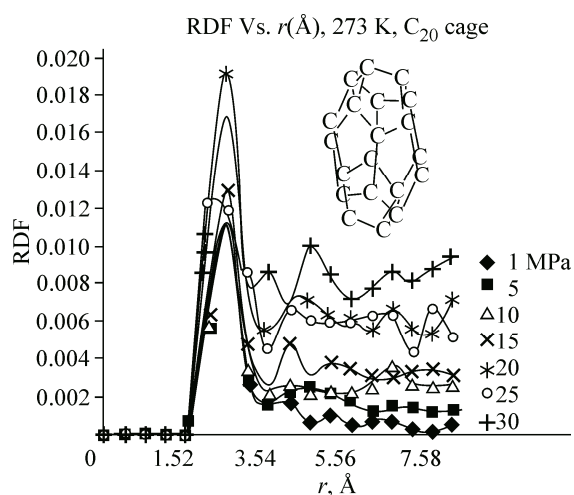


Fig. 1. Radial distribution function of C_{20(cage)}

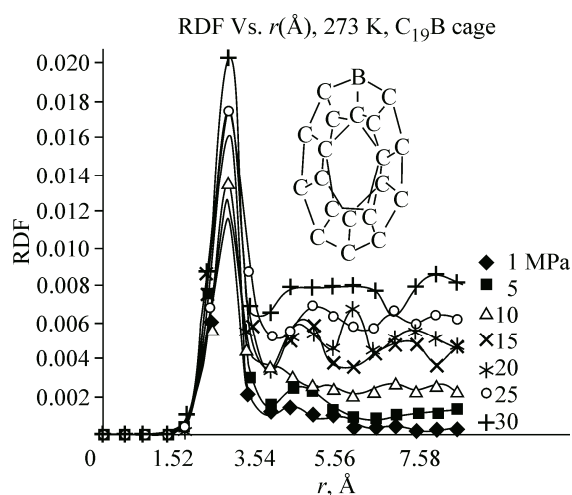
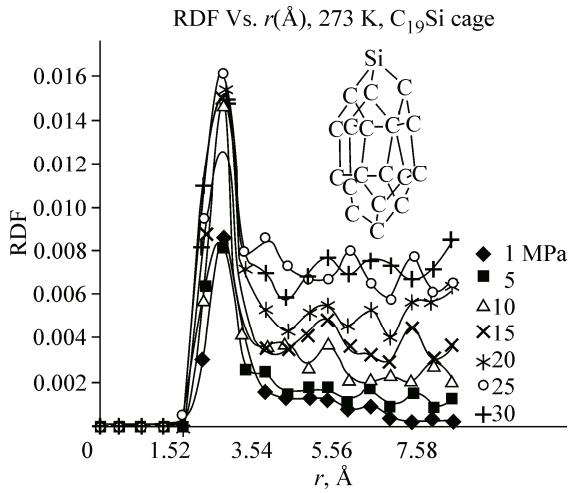


Fig. 2. Radial distribution function of C_{19B(cage)}

Fig. 3. Radial distribution function of $C_{19}Si_{(cage)}$

is 7.2 %, 7.6 % for $C_{19}B_{(cage)}$ at 273 K and 30 MPa, and 6.8 % of H_2 for $C_{19}Si_{(cage)}$ at 273 K and 25 MPa.

Conclusions. In this work, H_2 adsorption on $C_{20(cage)}$, $C_{19}B_{(cage)}$, and $C_{19}Si_{(cage)}$ fullerene structures have been investigated at different temperatures (273, 293, 320, and 400 K) for the pressure range between 1 and 30 MPa using the (N,V,T) Monte Carlo simulation. The results show that maximum RDF and ρ_w for the structures are obtained at 273 K and a pressure range between 20 and 30 MPa. The maximum value of RDF and ρ_w is obtained for $C_{19}B_{(cage)}$ at 273 K and 30 MPa with 0.020 % and 7.6 % of H_2 , respectively. This simulated result for $C_{19}B_{(cage)}$ is larger than the proposed value of the U. S. Department of Energy (DOE) Hydrogen plan, 6.5 wt% of H_2 .

Table 1

		RDF _{max} values at 3 Å					
		Structure					
T, K	$C_{20(cage)}$		$C_{19}B_{(cage)}$		$C_{19}Si_{(cage)}$		
	P, MPa	Maximum RDF	P, MPa	Maximum RDF	P, MPa	Maximum RDF	
273	25	0.01603	30	0.02018	20	0.01906	
298	5	0.01445	25	0.01561	10 (at 2.5 Å)	0.01459	
320	30	0.01558	10	0.01505	25	0.01602	
400	20	0.01463	5	0.01454	20	0.01648	

Table 2

Gravimetric storage capacity (ρ_w) of structures at different temperatures and pressures

P, MPa	Structure											
	$\rho_w C_{20(cage)}$				$\rho_w C_{19}B_{(cage)}$				$\rho_w C_{19}Si_{(cage)}$			
	T, K				T, K				T, K			
	273	298	320	400	273	298	320	400	273	298	320	400
1	0.0350	0.0414	0.0336	0.0284	0.0311	0.0364	0.0283	0.0317	0.0246	0.0249	0.0321	0.03182
5	0.0343	0.0462	0.0390	0.0366	0.0395	0.0415	0.0328	0.0473	0.0278	0.0449	0.0352	0.03099
10	0.0382	0.0521	0.0492	0.0428	0.0452	0.0421	0.0472	0.0391	0.0440	0.0370	0.0384	0.04781
15	0.0470	0.0473	0.0561	0.0510	0.0593	0.0500	0.0461	0.0482	0.0444	0.0405	0.0458	0.03998
20	0.0720	0.0492	0.0523	0.0522	0.0562	0.0434	0.0480	0.0473	0.0549	0.0441	0.0445	0.05064
25	0.0654	0.0677	0.0634	0.0483	0.0662	0.0621	0.0562	0.0462	0.0686	0.0580	0.0578	0.05354
30	0.0715	0.0673	0.0760	0.0573	0.0763	0.0627	0.0675	0.0540	0.0630	0.0587	0.0573	0.04787

REFERENCES

1. *Bisquert J.* // *J. Phys. Chem. Lett.* – 2011. – **2**. – P. 270 – 271.
2. *Zhou L.* *Renewable Sustainable Energy Rev.* – 2005. – **9**. – P. 395 – 408.
3. *Moriarty P., Honnery D.* // *Int. J. Hydrogen Energy.* – 2009. – **34**. – P. 31 – 39.
4. *Jena P.* // *J. Phys. Chem. Lett.* – 2011. – **2**. – P. 206 – 211.
5. *Melinon P., Masenelli B., Tournus F.* // *Nature Mater.* – 2007. – **6**. – P. 479 – 490.
6. *Ray A.K., Huda M.N.* // *J. Comput. Theor. Nanosci.* – 2006. – **3**. – P. 315 – 341.
7. *Kimura T., Sugai T., Shinohara H.* // *Chem. Phys. Lett.* – 1996. – **3**. – P. 269 – 273.
8. *Prinzbach H.* // *Nature.* – 2000. – **407**. – P. 60 – 63.
9. *Cheng J., Yuan X., Zhao L. et al.* // *Carbon.* – 2004. – **42**. – P. 2019 – 2024.
10. *Jia Y., Wang M., Wu L.* // *Sci. Technol.* – 2007 – **42**. – P. 3681 – 3695.
11. *Lithoxoos G., Samios J., Carissan Y.* // *J. Phys. Chem. C.* – 2008. – **112**. – P. 16725 – 16728.
12. *Sun W., Liu X., Wang Ch.* // *Acta Phys. Chim. Sin.* – 2009. – **58**. – P. 1126.
13. *Darkrim F., Levesque D.* // *J. Chem. Phys.* – 1998. – **109**. – P. 4981 – 4984.
14. *Lee S.M., Lee Y.H.* // *Appl. Phys. Lett.* – 2000. – **76**. – P. 2877 – 2879.
15. *Levesque D., Gicquel A., Darkrim F.L. et al.* // *J. Phys.: Condens. Matter.* – 2002. – **14**. – P. 9285 – 9293.
16. *Zheng H., Wang S., Cheng H.* // *Sci. China, Ser. B: Chem.* – 2004. – **47**. – P. 222 – 227.
17. *Cheng J., Zhang L., Ding R. et al.* // *Int. J. Hydrogen Energy.* – 2007. – **32**. – P. 3402 – 3405.
18. *Dimitrakakis G.K., Tylianakis E., Froudakis G.E.* // *Nano Lett.* – 2008. – **8**. – P. 3166 – 3170.
19. *Rafati A., Hashemianzadeh S.M., Bolboli Nojini Z. et al.* // *J. Comput. Chem.* – 2010. – **31**. – P. 1443 – 1449.